Heuristic Inspired Precoding for Millimeter-Wave MIMO Systems with Lens Antenna Subarrays

Sinasi Cetinkaya*, Liza Afeef †, Gokhan Mumcu*, Huseyin Arslan*†,
*Department of Electrical Engineering, Universityof South Florida, Tampa, FL, 33620
†Department of Electrical and Electronics Engineering, Istanbul Medipol University, Istanbul, TURKEY, 34810
e-mail: scetinkaya@usf.edu, liza.shehab@std.medipol.edu.tr, mumcu@usf.edu, arslan@usf.edu

***Abstract*—A traditional array (TA) multiple-input multiple-output (MIMO) architecture in mmWave with hybrid beamforming suffers from high power consumption and hardware overhead. Therefore, a lens antenna subarray (LAS)-MIMO architecture has been recently proposed as a promising technology for a power-efficient system and reducing hardware cost and complexity. Additionally, the LAS-MIMO can offer spectral efficiency (SE) performance close to TA-MIMO and higher than single-lens antenna array (SLA)-MIMO. In this paper, we propose a hybrid precoding algorithm for the LAS-MIMO in mmWave to efficiently control the LAS design. The precoding problem is formulated as a sparse reconstruction problem due to the sparse behavior of mmWave channel. The proposed algorithm is an iterative process developed jointly using artificial bee colony (ABC) optimization with orthogonal matching pursuit (OMP) algorithms. In each iteration, the algorithm first selects the switches for each lens randomly using ABC and then uses OMP to approximate optimal unconstrained precoders. This process continues until achieving maximum SE. The simulation results show that LAS has around a 30% increase in SE compared to SLA while providing a significant gain in energy efficiency (EE) for single radio-frequency (RF) chain and multi RF chain scenarios.**

***Index Terms*—Artificial bee colony optimization, basis pursuit, lens antenna subarray, precoding, MIMO.**

I. Introduction

Next-generation wireless communications are presumed to meet the demand for higher spectral efficiency (SE) (bits/s/Hz) and handle exponentially growing traffic volume [1]. To this end, less-congested millimeter-wave (mmWave) spectrum utilization is considered a promising solution to meet higher SE requirements and deal with enormous traffic demand [2]. A forte of mmWave frequencies is the ability to pack a large number of antenna elements into small physical areas due to smaller wavelengths. Hence, mmWave facilitates the use of massive multiple-input multiple-output (MIMO) which can overcome the severe free-space path loss due to high directional beamforming gain [3]. In addition, it is possible to enhance SE with massive MIMO by allowing multiple data streams with proper precoding techniques [4]. Typically, precoding in traditional-array (TA)-MIMO is performed digitally where each antenna element requires a dedicated radio-frequency (RF) chain resulting in huge cost and power consumption [5]. Therefore, the use of mmWave in MIMO systems makes hybrid analog and digital precoding preferable [6]–[8] which is performed by cascading a digital precoder in the baseband and an analog network between the RF chains and antenna elements. Hence, beam gain and interference management can be achieved simultaneously.

The analog network typically consists of phase shifters with combiners [9] or switches [10]. In massive MIMO systems, the use of an enormous number of phase shifters causes considerable hardware complexity along with signal processing complexity and power consumption, while the use of switches results in a significant performance loss. Accordingly, a promising research line is introduced by utilizing advanced antenna designs, such as single-lens antenna array (SLA) [11] and lens antenna subarray (LAS) [12], [13] to reduce signal processing complexity and RF chain cost without notable performance degradation. Due to the SLA-MIMO architecture's limitation including beamforming precoding/combining in a multipath channel and the large lens size that leads to high insertion loss and lack of scalability, the work in [13] presents an energy and spectral-efficient LAS-MIMO architecture. In the LAS-MIMO architecture shown in Fig. 1, each M antennas out of N antennas are connected to L small-sized lenses while the lenses are associated with a phase shifter network to control all the lenses together. For a specific lens, a simple switching network consisting of a single-pole multiple-throw (SPMT) switch controls the antenna elements. When the number of lenses is $L = 1$, the system falls to SLA-MIMO. On the other hand, the system performance is similar to the TA-MIMO when $L = N$. The LAS-MIMO provides better energy efficiency (EE) than the TA-MIMO with the expense of reducing the SE as L decreases. Hence, an appropriate precoding design is essential to enhance the SE.

Despite the attractive design of lens-aided MIMO systems, precoding design and beam selection problems remain an open issue, especially in LAS-MIMO, and they are not yet investigated, to the best of our knowledge. Therefore, in this paper, we take into account this problem. The contributions of this paper are summarized as follows:

- We propose a hybrid precoding algorithm for the LAS-MIMO based on artificial bee colony (ABC) and orthogonal matching pursuit (OMP) algorithms. It solves a non-convex optimization problem iteratively by exploiting the sparse characteristics of the mmWave channel.
- The SE and EE of the LAS architecture are investigated for a single user scenario with a single RF chain and multiple RF chains. As well, the EE performance is evaluated when different switch types (SP2T or SP4T)

are utilized.

Notation: $\mathbf{A}$, $\mathbf{a}$, a denote a matrix, a vector, and a scalar variable, respectively. $\|\mathbf{A}\|_F$ denotes $\mathbf{A}$'s Frobenius norm. $\mathbf{A}^*$, $\mathbf{A}^T$, $\mathbf{A}^{-1}$ are $\mathbf{A}$'s conjugate, transpose, and inverse respectively. $\mathrm{diag}(\mathbf{a})$ is a diagonal matrix with $\mathbf{a}$ on its diagonal. $\mathbf{I}$ is the identity matrix, and $\mathbb{C}^{M\times N}$ denotes the space of $M\times N$ complex-valued matrices. $\mathcal{CN}(\mu,\sigma^2)$ is a complex Gaussian random vector with mean μ and covariance σ^2. j is the imaginary unit of complex numbers with $j^2=-1$.

II. System Model

This section introduces the radio environment, SE, and power consumption model of the LAS-MIMO architecture.

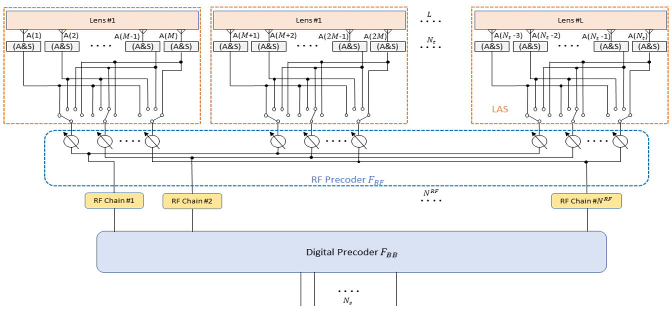

Fig. 1: Hybrid precoding for LAS-MIMO architecture

A. Radio Environment and Parameters

We consider a single-user LAS-MIMO operating at mmWave frequencies where the transmitter employs N_t antennas connected to L_t lenses to transmit N_s data streams to a receiver equipped with N_r phased antenna array. Multi-stream communication is enabled by employing the transmitter with N_t^{RF} RF chains where $N_s\leq N_t^{\mathrm{RF}}\leq N_t$. According to hybrid precoding presented in Fig. 1, the received signal is given as

$$\mathbf{r}=\sqrt{\rho}\mathbf{HFs}+\mathbf{n}, \tag{1}$$

where $\mathbf{r}\in\mathbb{C}^{N_r\times 1}$ is the received signal, ρ is the average received signal power, $\mathbf{H}\in\mathbb{C}^{N_r\times N_t}$ is the channel matrix, and $\mathbf{F}\in\mathbb{C}^{N_t\times N_s}$ is the precoder matrix. The transmitted data $\mathbf{s}\in\mathbb{C}^{N_s\times 1}$ has the normalized power of $\mathbb{E}[\mathbf{ss}^*]=\mathbf{I}_{N_s}$. Additionally, the additive white Gaussian noise (AWGN) with zero mean and variance σ^2 is modeled as $\mathbf{n}\sim\mathcal{CN}(0,\sigma^2)$. The precoding matrix is expressed as $\mathbf{F}=\mathbf{F}_{\mathrm{Lens}}^{\mathbf{m}}\mathbf{F}_{\mathrm{RF}}\mathbf{F}_{\mathrm{BB}}$ where $\mathbf{F}_{\mathrm{Lens}}^{\mathbf{m}}\in\mathbb{C}^{N_t\times L_t}$ is the lens antenna effect for a given $\mathbf{m}\in\mathbb{C}^{1\times L_t}$ vector containing the selected antenna indexes [13], $\mathbf{F}_{\mathrm{RF}}\in\mathbb{C}^{L_t\times N_t^{\mathrm{RF}}}$ is the analog beamformer obtained by the phase shifters, and $\mathbf{F}_{\mathrm{BB}}\in\mathbb{C}^{N_t^{\mathrm{RF}}\times N_s}$ is the digital baseband precoder where the total transmit power constraint is normalized such that $||\mathbf{F}_{\mathrm{Lens}}^{\mathbf{m}}\mathbf{F}_{\mathrm{RF}}\mathbf{F}_{\mathrm{BB}}||_F^2=N_s$ [5]. Due to the subarray structure of the LAS-MIMO, no contribution among subarrays is obtained [13]. Therefore, each column of the $\mathbf{F}_{\mathrm{Lens}}^{\mathbf{m}}$ matrix contains zeros and $\mathbf{v}^{\mathbf{m}}$ vector representing the selected beam from each lens [13], and is given as

$$\mathbf{F}_{\mathrm{Lens}}^{\mathbf{m}}=\begin{bmatrix}\mathbf{v}^{\mathbf{m(1)}} & \mathbf{0}_{M\times 1} & \dots & \mathbf{0}_{M\times 1}\\ \mathbf{0}_{M\times 1} & \mathbf{v}^{\mathbf{m(2)}} & \mathbf{0}_{M\times 1} & \\ \vdots & & \ddots & \\ \mathbf{0}_{M\times 1} & \dots & \mathbf{0}_{M\times 1} & \mathbf{v}^{\mathbf{m(L_t)}}\end{bmatrix}_{N_t\times L_t}, \tag{2}$$

where M denotes the number of antennas placed under each lens and $\mathbf{v}^{\mathbf{m}}=[e^{-jkd\sin(\theta_m)\Omega}]_{\Omega\in\mathcal{I}(M)}$, where $\mathcal{I}(M)=\{q-(M-1)/2, q=0,1,\dots,M-1\}$, $k=\frac{2\pi}{\lambda}$, d is the antenna element spacing, λ is signal wavelength and $\theta_m=\frac{\pi}{4}-\frac{\pi(m-1)}{2(M-1)}$ is the metric showing the direction of the radiating beam from LAS for a given antenna element $m=1,2,...,M$ chosen by the switch network [13].

We adopt a narrowband clustered channel model for the channel matrix $\mathbf{H}$, based on the Saleh-Valenzuela model, in order to capture the characteristics of the mmWave MIMO channel precisely [5], [14]–[16] which is expressed as [17]

$$\mathbf{H}=\sqrt{\frac{N_tN_r}{N_{cl}N_{ray}}}\sum_{i=1}^{N_{cl}}\sum_{k=1}^{N_{ray}}\gamma_{i,k}\mathbf{a_r}(\phi_{i,k})\mathbf{a_t}^*(\theta_{i,k}), \tag{3}$$

where $\gamma_{i,k}$ stands for the complex gain of the k^{th} ray in the i^{th} scattering cluster. The angle of departure (AoD) and angle of arrival (AoA) for the k^{th} ray in the i^{th} scattering cluster are defined by $\theta_{i,k}$ and $\phi_{i,k}$, respectively. The received and transmitted array response vectors are represented by $\mathbf{a_r}(\phi_{i,k})$ and $\mathbf{a_t}(\theta_{i,k})$, respectively. Considering an N-element uniform linear array (ULA), the array response vector for a given $\psi\in\{\theta,\phi\}$ can be stated as $\mathbf{a}(\psi)=\frac{1}{\sqrt{N}}\left[1,e^{jkd\sin(\psi)},\dots,e^{j(N-1)kd\sin(\psi)}\right]^T$ [18].

B. Spectral Efficiency and Power Consumption of LAS Hybrid MIMO Architecture

In this work, we assume that the transmitter is equipped with LAS and the receiver is equipped with no LAS. Considering the ULA, the combiner can be stated as $\mathbf{W}=\mathbf{W}_{\mathrm{RF}}\mathbf{W}_{\mathrm{BB}}$ [19] where $\mathbf{W}_{\mathrm{RF}}\in\mathbb{C}^{N_r\times N_r^{\mathrm{RF}}}$ is the analog combiner obtained by the phase shifters, and $\mathbf{W}_{\mathrm{BB}}\in\mathbb{C}^{N_r^{\mathrm{RF}}\times N_s}$ is the digital baseband combiner. Additionally, the number of RF chains at the receiver is defined by N_r^{RF}.

Assuming that the base station can obtain perfect channel state information (CSI), the average SE for the LAS-MIMO can be deriven from [5] and [13] and given as

$$R=\log_2\left(\mathbf{I}_{N_s}+\frac{\rho}{N_s}\mathbf{R_n}^{-1}\mathbf{W}^*\mathbf{HFF}^*\mathbf{H}^*\mathbf{W}\right), \tag{4}$$

where $\mathbf{R_n}=\sigma^2\mathbf{W}^*\mathbf{W}$ stands for the noise variance matrix.

The LAS-MIMO architecture aims to reduce power consumption and hardware complexity by connecting each RF chain to each lens through one phase shifter and one switch. In contrast, the hybrid TA-MIMO requires all the RF chains to be connected to each antenna element through a phase shifter. Therefore, an accurate power consumption model for the LAS-MIMO transmitter is derived in [13] as $P_t^{LAS}=\frac{P_{T_x}^{LAS}}{(\eta_{PA}\eta_{SW})}+N_t^{\mathrm{RF}}(LP_{PS}+LN_{SW}P_{SW}+P_{RF})$, where $P_{T_x}^{LAS}$, P_{PS}, P_{SW}, and P_{RF} stand for the transmit power consumption in the LAS system, the power consumption of a phase shifter, a switch, and an RF chain, respectively. Additionally, η_{PA} and $\eta_{\mathrm{SW}}=10^{-\zeta\mathrm{IL_{SW}}/10}$ stand for the efficiency of the transmitted amplifiers, and the efficiency of the switches, respectively. ζ is the number of series switches needed to be placed under each lens and $\mathrm{IL_{SW}}$ is the insertion loss for a switch.

Another performance metric that needs to be defined is EE which is defined as the number of bits that can be transmitted per unit of energy [20] and expressed as $EE = R/P_t^{LAS}$ (bps/Hz/W) for the LAS architecture.

III. Problem Formulation

For simplicity and tractability of the optimization problem, we consider only designing hybrid precoders $\mathbf{F}_{\text{Lens}}^{\mathbf{m}}\mathbf{F}_{\text{RF}}\mathbf{F}_{\text{BB}}$ since joint optimization of hybrid precoders and combiners $\mathbf{W}_{\text{RF}}\mathbf{W}_{\text{BB}}$ are unlikely due to the non-convex constraints caused by phase shifters and switches [5]. Note that, the hybrid combiner design will be investigated as future work. Since our goal is designing only the hybrid precoders, the equation (4) needs to be rewritten as

$$R = \log_2\left(\mathbf{I}_{N_s} + \frac{\rho}{N_s\sigma^2}\mathbf{H}\mathbf{F}\mathbf{F}^*\mathbf{H}^*\right), \tag{5}$$

Given equation (5), the optimization problem is formulated as

$$(\mathbf{F}_{\text{Lens}}^{\text{opt}}, \mathbf{F}_{\text{RF}}^{\text{opt}}, \mathbf{F}_{\text{BB}}^{\text{opt}}) = \underset{\mathbf{F}_{\text{Lens}}^{\mathbf{m}}, \mathbf{F}_{\text{RF}}, \mathbf{F}_{\text{BB}}}{\text{argmax}}\ R, \tag{6a}$$
$$\text{s.t.}\quad \mathbf{F}_{\text{Lens}}^{\mathbf{m}} \in \mathcal{F}_{\text{Lens}}, \tag{6b}$$
$$\mathbf{F}_{\text{RF}} \in \mathcal{F}_{\text{RF}}, \tag{6c}$$
$$||\mathbf{F}_{\text{Lens}}^{\mathbf{m}}\mathbf{F}_{\text{RF}}\mathbf{F}_{\text{BB}}||_F^2 = N_s, \tag{6d}$$

where $\mathcal{F}_{\text{Lens}}$ and $\mathcal{F}_{\text{RF}}$ stand for the set containing all the feasible lens antenna effects and the set of feasible RF precoders, respectively.

The problem given in (6) is a challenging optimization problem due to its non-convex amplitude constraints in (6b) and (6c). Although no optimal solution methodology exists for the problem (6) [5], an approximation is proposed in [5] to provide a near-optimal solution and proved that the maximization problem (6) is equivalent to the minimization problem of the distance between optimal unconstrained singular value decomposition (SVD) based precoder $\mathbf{F}_{\text{opt}}$ and practical hybrid precoder. Thus, the problem (6) can be rewritten as

$$(\mathbf{F}_{\text{Lens}}^{\text{opt}}, \mathbf{F}_{\text{RF}}^{\text{opt}}, \mathbf{F}_{\text{BB}}^{\text{opt}}) = \underset{\mathbf{F}_{\text{Lens}}^{\mathbf{m}}, \mathbf{F}_{\text{RF}}, \mathbf{F}_{\text{BB}}}{\text{argmin}}\ ||\mathbf{F}_{\text{opt}} - \mathbf{F}_{\text{A}}\mathbf{F}_{\text{BB}}||_F, \tag{7a}$$
$$\text{s.t.}\quad \text{(6b) to (6d)}, \tag{7b}$$

where $\mathbf{F}_{\text{A}} = \mathbf{F}_{\text{Lens}}^{\mathbf{m}}\mathbf{F}_{\text{RF}}$ stands for the total analog precoder which is the matrix multiplication of lens antenna effect and RF precoder. There is a relationship between the analog part of the precoder $\mathbf{F}_{\text{A}}$ and the transmit antenna array response vector $\mathbf{a_t}(\theta_{i,k})$ where the sparse-scattering structure of mmWave can be exploited to represent $\mathbf{F}_{\text{A}}$ as a function of $\mathbf{a_t}(\theta_{i,k})$ [5]. Considering that, equation (7) can be modified as

$$(\mathbf{F}_{\text{Lens}}^{\text{opt}}, \mathbf{F}_{\text{RF}}^{\text{opt}}, \mathbf{F}_{\text{BB}}^{\text{opt}}) = \underset{\mathbf{F}_{\text{Lens}}^{\mathbf{m}}, \mathbf{F}_{\text{RF}}, \mathbf{F}_{\text{BB}}}{\text{argmin}}\ ||\mathbf{F}_{\text{opt}} - \mathbf{F}_{\text{A}}\mathbf{F}_{\text{BB}}||_F, \tag{8a}$$
$$\text{s.t.}\quad {\mathbf{F}_{\text{A}}}^{(i)} \in \{\mathbf{a_t}(\theta_{i,k}), \forall i,k\}, \tag{8b}$$
$$\mathbf{F}_{\text{A}} = \mathbf{F}_{\text{Lens}}^{\mathbf{m}}\mathbf{F}_{\text{RF}}, \tag{8c}$$
$$||\mathbf{F}_{\text{A}}\mathbf{F}_{\text{BB}}||_F^2 = N_s. \tag{8d}$$

The precoding design for the LAS-MIMO requires a switch selection step to find the best beam selected from each lens since the lens antenna effect $\mathbf{F}_{\text{Lens}}^{\mathbf{m}}$ depends on the position of the activated switches. Therefore, the proposed precoding design first selects the $\mathbf{m}$ vector containing the selected beam indexes then find the $\mathbf{F}_{\text{RF}}$ and $\mathbf{F}_{\text{BB}}$ accordingly. This iterative process continues until finding the optimum precoders. Hence, $\mathbf{F}_{\text{Lens}}^{\mathbf{m}}$ can be omitted for a given $\mathbf{m}$ in each iteration, while ${\mathbf{F}_{\text{A}}}^{(i)}$ in (8b) can be embedded into the optimization problem due to the direct relationship between ${\mathbf{F}_{\text{A}}}^{(i)}$ and $\mathbf{a_t}(\theta_{i,k})$ [5]. Hence, the optimization problem becomes

$$(\tilde{\mathbf{F}}_{\text{RF}}^{\text{opt}}, \tilde{\mathbf{F}}_{\text{BB}}^{\text{opt}}) = \underset{\tilde{\mathbf{F}}_{\text{RF}}, \tilde{\mathbf{F}}_{\text{BB}}}{\text{argmin}}||\mathbf{F}_{\text{opt}} - \mathbf{A_t}\tilde{\mathbf{F}}_{\text{BB}}||_F, \tag{9a}$$
$$\text{s.t.}\quad ||\text{diag}(\tilde{\mathbf{F}}_{\text{BB}}\tilde{\mathbf{F}}_{\text{BB}}^*)||_0 = N_{\text{t}}^{\text{RF}}, \tag{9b}$$
$$\mathbf{F}_{\text{Lens}}^{\mathbf{m}}\tilde{\mathbf{F}}_{\text{RF}} = \mathbf{A_t}, \tag{9c}$$
$$||\mathbf{A_t}\tilde{\mathbf{F}}_{\text{BB}}||_F^2 = N_s, \tag{9d}$$

where $\mathbf{A_t} = [\mathbf{a_t}(\theta_{1,1}), \ldots, \mathbf{a_t}(\theta_{N_{cl},N_{ray}})] \in \mathbb{C}^{N_t \times N_{cl}N_{ray}}$ stands for the array response vector which is also the auxiliary variable obtained from $\mathbf{F}_{\text{A}}$ while the auxiliary variables for $\mathbf{F}_{\text{BB}}$ and $\mathbf{F}_{\text{RF}}$ are given as $\tilde{\mathbf{F}}_{\text{BB}}$ and $\tilde{\mathbf{F}}_{\text{RF}}$, respectively [5].

IV. Solution of the Problem

This section proposes a hybrid beamforming algorithm to solve the NP-hard and non-convex problem (9). Consequently, we propose a swarm-based heuristic algorithm, namely ABC aided spatially sparse precoding. It deploys both ABC and OMP by exploiting the sparse scattering characteristics of the mmWave channel. It is also possible to consider other existing swarm-based optimization tools (i.e., particle swarm optimization (PSO) [21] and ant colony optimization (ACO) [22]). However, they are likely to fall into a local minimum or optimum solution region and be stuck there [23] if a problem has non-convexity properties. Therefore, ABC is more suitable since finding the global optimum solution rather than the local optimum solution is its strength [23], [24]. Another reason for selecting ABC is that it can be easily implemented in real-time applications due to its minimum parameter requirements for tuning and its fast convergence ability [25].

ABC is inspired by the food search behavior of the honey bees and proposed by Karaboga [26] in 2005. In a bee swarm, food sources define the possible solutions the nectar amount of a food source represents the quality (fitness) of the food source. The number of food sources is equal to half of the population. The algorithm consists of four phases: initialization phase, employed bees phase, onlooker bees phase, and scout bees phase. The proposed solution of problem (9) is presented in Algorithm 1.

1) Initialization Phase: We randomly initialize the food sources (selected antenna indexes) $\mathbf{m}_i$'s such that $i \in \{1, \ldots, S\}$ where S is the population size. Since the antenna selection is an integer programming problem, the initial solutions have to be integer values where $1 \leq \mathbf{m}_i \leq M$ and can be produced by

$$\mathbf{m}_{ij} = round(\mathbf{m}_j^{\text{max}} + rand(0,1) \times (\mathbf{m}_j^{\text{max}} - \mathbf{m}_j^{\text{min}})), \tag{10}$$

where $j \in \{1, 2, \ldots, L_t\}$, $\mathbf{m}_j^{\text{min}} = 1$, and $\mathbf{m}_j^{\text{max}} = M$. Then, the corresponding $\mathbf{F}_{\text{Lens}}^{\mathbf{m}_i}$ is found using (2). $\mathbf{F}_{\text{Lens}}^{\mathbf{m}_i}$, and randomly generated $\mathbf{F}_{\text{RF}}$ and $\mathbf{F}_{\text{BB}}$ are used to calculate the SE using (5) to find the best solution $\mathbf{m}^{\mathbf{best}}$ providing the highest SE at this time.

2) Employed Bee Phase: The bees look for new possible solutions providing better results than the results kept in their memory. The possible solutions in the neighborhood are given as

$$\mathbf{v}_{ij} = round(\mathbf{m}_{ij} + \alpha_{ij} \times (\mathbf{m}_{ij} - \mathbf{m}_{kj})), \tag{11}$$

where i and $k \in \{1, \ldots, S\}$ are randomly chosen indexes and $k \neq i$. $\alpha_{ij} \in [-1, 1]$ is a control parameter and responsible of keeping the newly produced solutions around $\mathbf{m}_{ij}$. After the search procedure is completed, $\mathbf{F}_{\text{Lens}}^{\mathbf{m}_i}$ is calculated using (2). Then, $\mathbf{F}_{\text{Lens}}^{\mathbf{m}_i}$ is sent to Algorithm 2 to calculate $\mathbf{F}_{\text{RF}}$ and $\mathbf{F}_{\text{BB}}$ guaranteeing the objective function given in (9). Accordingly, a greedy selection is applied between $\mathbf{v}_i$ and $\mathbf{m}_i$ using (5) to find the better solutions. After the selection, $\mathbf{m}_i$ is updated and the fitness function of using $\mathbf{m}_i$ are calculated as

$$\mathbf{F}_i = \begin{cases} \frac{1}{1+g(\mathbf{m}_i)}, & g(\mathbf{m}_i) \geq 0 \\ 1 + \text{abs}\left(g(\mathbf{m}_i)\right), & \text{otherwise} \end{cases}, \tag{12}$$

where $g(\mathbf{m}_i)$ is the objective function of the updated solution vector.

3) Onlooker Bee Phase: According to the solution vector and their fitness values shared by the employed bees, onlooker bees select their solution based on a probabilistic model which uses the fitness function given as $p_i = \mathbf{F}_i / \sum_i^S \mathbf{F}_i$. After new solutions are selected, the onlooker bees update their position using (11) and fitness function using (12) accordingly.

4) Scout Bee Phase: The bees replace the abandoned solutions, not improved for a particular number of trials, with new randomly generated possible solutions using (10). Bees memorize all these steps and share them, and the algorithm runs until it reaches the maximum number of iterations.

Algorithm 1: ABC Aided Hybrid Sparse Precoding

Input: $\mathbf{F}_{\text{opt}}$, and $\mathbf{A_t}$.
ABC parameters: $S = 100$, $i_{max} = 500$.
Output: $\mathbf{F}_{\text{Lens}}^{\mathbf{m}}$, $\mathbf{F}_{\text{RF}}$, $\mathbf{F}_{\text{BB}}$.
1 Randomly generate S solutions $\mathbf{m}_i$ using (10),
2 Calculate $\mathbf{F}_{\text{Lens}}^{\mathbf{m}_i}$ using (2),
3 Randomly generate $\mathbf{F}_{\text{RF}}$ and $\mathbf{F}_{\text{BB}}$,
4 Evaluate the function using (5), and select $\mathbf{m}^{\mathbf{best}}$,
5 **while** $i < i_{max}$ **do**
6 (Phase-1: Employed Bee Phase)
7 **for** $s = 1 : S$ **do**
8 Produce a new solutions $\mathbf{v}_i$ using (11) and calculate corresponding $\mathbf{F}_{\text{Lens}}^{\mathbf{v}_i}$ as in (2),
9 Calculate $\mathbf{F}_{\text{RF}}$ and $\mathbf{F}_{\text{BB}}$ using **Algorithm 2**,
10 Evaluate the function using (5), and apply greedy selection between $\mathbf{v}_i$ and $\mathbf{m}_i$,
11 Update $\mathbf{m}_i$ and find fitness function using (12),
end
12 (Phase-2: Onlooker Bee Phase)
13 **for** $s = 1 : S$ **do**
14 Find the selection probabilities p_i,
15 Use p_i to generate new solutions $\mathbf{v}_i$ from $\mathbf{m}_i$
16 Select a food source vector $\mathbf{m}^{\text{curr}}$ according to p_s value,
17 Follow same steps from step-9 to step-11.
end
18 (Phase-3: Scout Bee Phase)
19 **for** $s = 1 : S$ **do**
20 Identify the abandoned solutions not improved after a predetermined number of trials,
21 Replace them with new randomly generated solutions using (10),
22 Store the best solution ever found,
end
end
23 **return** $\mathbf{F}_{\text{Lens}}^{\mathbf{m}}$, $\mathbf{F}_{\text{RF}}$, $\mathbf{F}_{\text{BB}}$.

V. Simulation Results

This section illustrates the SE and EE performance of the proposed algorithm for the hybrid LAS-MIMO in mmWave. The TA-MIMO and SLA-MIMO are chosen as the baseline architectures for fair performance comparison. The power consumption model is evaluated utilizing switch types of SP2T and SP4T to compare the EE performance. In the simulation, the channel parameters are set to $N_{cl} = 6$, $N_{ray} = 8$, $f_c = 38$ GHz, and 500 MHz bandwidth. Furthermore, AoAs and AoDs are uniformly distributed over $[-\frac{\pi}{4}, \frac{\pi}{4}]$ and $[-\frac{\pi}{2}, \frac{\pi}{2}]$, respectively [27]. It is assumed that we have a downlink MIMO scenario where the precoding is designed using the proposed algorithm and the combiner is designed using the algorithm in [28], while the CSI is assumed to be perfectly known. The results are averaged over 500 channel realizations. The rest of simulation parameters are listed in Table 1.

Fig. 2a shows the SE of 64×16 LAS-MIMO and TA-MIMO architectures with a single RF chain. The proposed algorithm provides better performance in the LAS-MIMO ($L = 4, 8, 16$) than in the SLA-MIMO ($L = 1$) as the number of lenses increases in the array. More precisely, the SE is almost enhanced by 16%, 24% and 35% for $L = 4$, $L = 8$ and $L = 16$, respectively at $SNR = 5$ dB. In the simulation, we inspired and modified the spatially sparse precoding algorithm in [5], which performs very close to the optimal unconstrained SVD precoding, to present the simulation results for the TA-MIMO. The results show that TA-MIMO outperforms all LAS-MIMO scenarios due to its high precoding capability.

For the same system configurations, the EE analysis is shown in Fig. 2b where the proposed algorithm provides better performance in the LAS-MIMO than the TA-MIMO and SLA-MIMO as the number of lenses increases. Using SP4T switches in the switching network shows some enhancement in the performance rather than using SP2T switches. In particular, $L = 16$ outperforms all others while SLA ($L = 1$) has the worst performance among others when SP2T switch type is used to implement LAS-MIMO. On the other hand, $L = 4$ becomes the winner in EE due to the reduced number of

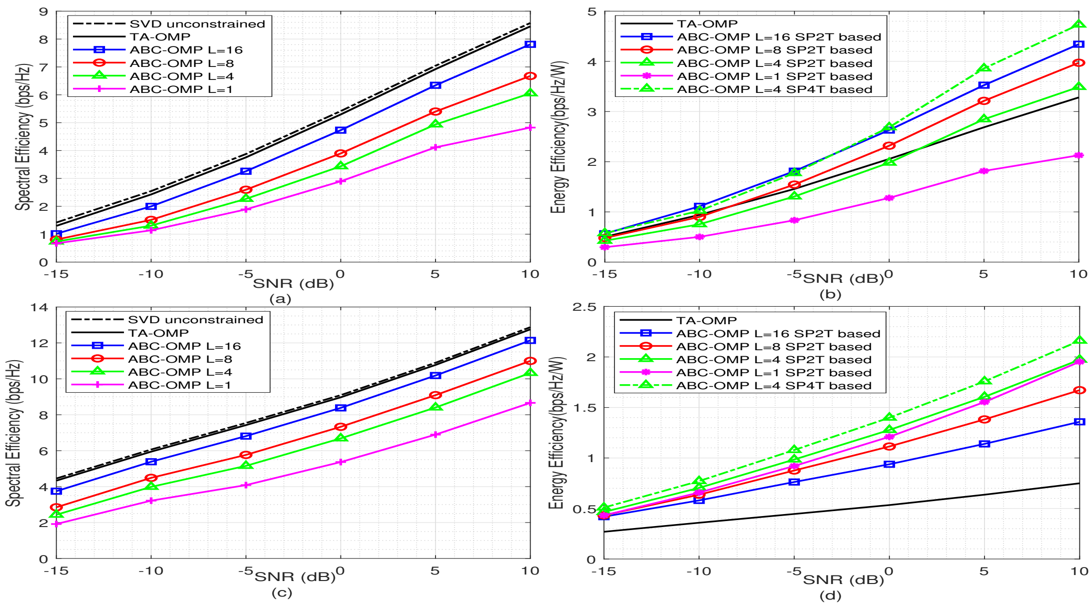

Fig. 2: Performance comparison of TA-MIMO and LAS-MIMO with various algorithms. (a) and (c) Spectral efficiency vs SNR for $N_{\text{RF}} = 1$ and $N_{\text{RF}} = 8$, respectively, (b) and (d) Energy efficiency vs SNR for $N_{\text{RF}} = 1$ and $N_{\text{RF}} = 8$, respectively.

switches and switch insertion loss when SP4T switch type is utilized. Although we obtain a high precoding gain with the ABC-OMP algorithm, it is essential to note that the LAS requires a careful design to make a fair decision between SE and EE trade-off.

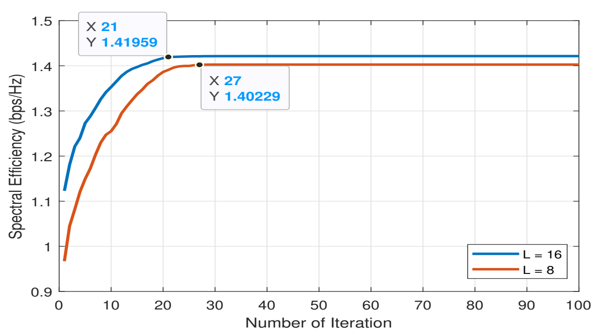

Fig. 3: Convergence rate of ABC-OMP algorithm

TABLE I: SIMULATION PARAMETERS

Parameters	Value
Power consumption of a phase shifter (P_{PS})	30 mW [10]
Power consumption of an SP2T switch (P_{SP2T})	10 mW [13]
Power consumption of an SP4T switch (P_{SP4T})	20 mW [13]
P_{RF}	220 mW [13]
η_{PA}	0.2 [13]
IL_{SW}	1 dB [13]

Multi RF chain scenarios are evaluated in Fig. 2c and Fig. 2d showing SE and EE, respectively. The proposed algorithm provides satisfactory results even with $N_t = 64$, $N_r = 16$, and $N_t^{\text{RF}} = 8$ scenario. Since the precoding capability increases when the number of lenses increases, $L = 16$ still outperforms all the other LAS architectures with 32% more SE at $SNR = 5$ dB than SLA. On the other hand, Fig. 2d shows that LAS-MIMO with $L = 4$ provides the best performance in EE when SP2T switches are utilized. However, the performance can further be enhanced with SP4T switches. Specifically, using SP4T switch instead of SP2T switch provides 9% more EE at $SNR = 5$ dB. For $L = 16$ and $L = 8$ architectures, the reason for having worse performance than the SLA architecture is that the number of required phase shifters and switches increases as N_t^{RF} increases, causing higher power consumption.

The SE and EE analysis of the proposed algorithm indicates that the LAS-MIMO with $L = 16$ and SP2T switches provides the optimum performance compared to other systems (SLA and TA-MIMO) when $N_t^{\text{RF}} = 1$. In multi RF scenarios, LAS-MIMO offers the best EE and SE when $L = 4$, and $L = 16$, respectively. Thus, one can design the system depending on the EE and SE trade-off to provide optimum performance based on the system requirements.

Finally, the convergence property of the proposed algorithm is presented in Fig. 3 when $SNR = 5$ dB. The algorithm is run for 100 iterations for the same channel configuration, and the convergence rate is averaged. We can see that it quickly converges after almost 21 iterations when $L = 16$ and 27 iterations when $L = 8$.

VI. Conclusion

In this paper, we propose a hybrid precoding algorithm for mmWave LAS-MIMO architectures that uses the heuristic ABC and OMP algorithms. Thus, it is called ABC-aided spatially sparse precoding. The proposed precoding algorithm first selects the antennas that need to be activated for each lens and calculates the corresponding lens antenna effect. This information is then used in OMP to find the analog and digital precoders where the precoding problem is formulated as a sparse reconstruction problem due to the sparse behavior of the

Algorithm 2: Spatially Sparse Precoding

Input: $\mathbf{A_t}$, $\mathbf{F}_{\text{opt}}$, and $\mathbf{F}^{\mathbf{m}}_{\text{Lens}}$.

Output: $\mathbf{F}_{\text{RF}}$, and $\mathbf{F}_{\text{BB}}$.

$\mathbf{F}_{\text{A}} =$ Empty Matrix, and $\mathbf{F_{res}} = \mathbf{F}_{\text{opt}}$,

for $i = 1 : N_t^{RF}$ **do**

$\quad \mathbf{\Psi} = \mathbf{A_t}^* \mathbf{F_{res}}$,

$\quad k = \text{argmax}_{l=1,\dots,N_{cl}N_{ray}} (\mathbf{\Psi}\mathbf{\Psi}^*)_{l,l}$,

$\quad \mathbf{F}_{\text{A}} = [\mathbf{F}_{\text{A}} | \mathbf{A_t^{(k)}}]$,

$\quad \mathbf{F}_{\text{RF}} = (\mathbf{F}^{\mathbf{m}}_{\text{Lens}}{}^* \mathbf{F}^{\mathbf{m}}_{\text{Lens}})^{-1} \mathbf{F}^{\mathbf{m}}_{\text{Lens}}{}^* \mathbf{F}_{\text{A}}$,

$\quad \mathbf{F}_{\text{BB}} = (\mathbf{F}_{\text{A}}{}^* \mathbf{F}_{\text{A}})^{-1} \mathbf{F}_{\text{A}}{}^* \mathbf{F}_{\text{opt}}$,

$\quad \mathbf{F_{res}} = \frac{\mathbf{F}_{\text{opt}} - \mathbf{F}^{\mathbf{m}}_{\text{Lens}} \mathbf{F}_{\text{RF}} \mathbf{F}_{\text{BB}}}{||\mathbf{F}_{\text{opt}} - \mathbf{F}^{\mathbf{m}}_{\text{Lens}} \mathbf{F}_{\text{RF}} \mathbf{F}_{\text{BB}}||_F}$,

end

$\mathbf{F}_{\text{BB}} = \sqrt{N_s} \frac{\mathbf{F}_{\text{BB}}}{||\mathbf{F}^{\mathbf{m}}_{\text{Lens}} \mathbf{F}_{\text{RF}} \mathbf{F}_{\text{BB}}||_F}$,

return $\mathbf{F}_{\text{RF}}$, $\mathbf{F}_{\text{BB}}$

mmWave channel. ABC runs until it finds the best precoding components providing the highest SE. The simulation results show that it can achieve near-optimal performance in terms of SE as the number of lenses increases in the LAS system while outperforming the TA-MIMO in terms of EE for single and multiple RF chains. Additionally, using different switch types may further improve the EE while maintaining the same SE. The future scope of this work can be proposing an algorithm that can handle joint precoding and combining for a multi-user scenario.

VII. Acknowledgement

This material is based upon work supported by the National Science Foundation under Grant ECCS-1923857.

References

[1] V. K. Trivedi, K. Ramadan, P. Kumar, M. I. Dessouky, and F. E. Abd El-Samie, "Enhanced OFDM-NOMA for next generation wireless communication: a study of PAPR reduction and sensitivity to CFO and estimation errors," *AEU-International Journal of Electronics and Communications*, vol. 102, pp. 9–24, 2019.

[2] M. M. Lodro, N. Majeed, A. A. Khuwaja, A. H. Sodhro, and S. Greedy, "Statistical channel modelling of 5G mmWave MIMO wireless communication," in *2018 International Conference on Computing, Mathematics and Engineering Technologies (iCoMET)*. IEEE, 2018, pp. 1–5.

[3] J. Huang, C.-X. Wang, R. Feng, J. Sun, W. Zhang, and Y. Yang, "Multi-frequency mmWave massive MIMO channel measurements and characterization for 5G wireless communication systems," *IEEE Journal on Selected Areas in Communications*, vol. 35, no. 7, pp. 1591–1605, 2017.

[4] D. J. Love and R. W. Heath, "Multimode precoding for MIMO wireless systems," *IEEE Transactions on Signal Processing*, vol. 53, no. 10, pp. 3674–3687, 2005.

[5] O. E. Ayach, S. Rajagopal, S. Abu-Surra, Z. Pi, and R. W. Heath, "Spatially sparse precoding in millimeter wave MIMO systems," *IEEE Transactions on Wireless Communications*, vol. 13, no. 3, pp. 1499–1513, 2014.

[6] X. Gao, L. Dai, S. Han, I. Chih-Lin, and R. W. Heath, "Energy-efficient hybrid analog and digital precoding for mmWave MIMO systems with large antenna arrays," *IEEE Journal on Selected Areas in Communications*, vol. 34, no. 4, pp. 998–1009, 2016.

[7] I. Ahmed, H. Khammari, A. Shahid, A. Musa, K. S. Kim, E. De Poorter, and I. Moerman, "A survey on hybrid beamforming techniques in 5G: Architecture and system model perspectives," *IEEE Communications Surveys & Tutorials*, vol. 20, no. 4, pp. 3060–3097, 2018.

[8] Z. Pi and F. Khan, "An introduction to millimeter-wave mobile broadband systems," *IEEE communications magazine*, vol. 49, no. 6, pp. 101–107, 2011.

[9] F. Sohrabi and W. Yu, "Hybrid digital and analog beamforming design for large-scale antenna arrays," *IEEE Journal of Selected Topics in Signal Processing*, vol. 10, no. 3, pp. 501–513, 2016.

[10] R. Mendez-Rial, C. Rusu, N. González-Prelcic, A. Alkhateeb, and R. W. Heath, "Hybrid MIMO architectures for millimeter wave communications: Phase shifters or switches?" *IEEE Access*, vol. 4, pp. 247–267, 2016.

[11] J. Brady, N. Behdad, and A. M. Sayeed, "Beamspace MIMO for millimeter-wave communications: System architecture, modeling, analysis, and measurements," *IEEE Transactions on Antennas and Propagation*, vol. 61, no. 7, pp. 3814–3827, 2013.

[12] M. Karabacak, G. Mumcu, and H. Arslan, "Hybrid MIMO architecture using lens arrays," Jul. 14 2020, US Patent 10,714,836.

[13] M. Karabacak, H. Arslan, and G. Mumcu, "Lens antenna subarrays in mmWave hybrid MIMO systems," *IEEE Access*, vol. 8, pp. 216 634–216 644, 2020.

[14] A. Forenza, D. J. Love, and R. W. Heath, "Simplified spatial correlation models for clustered MIMO channels with different array configurations," *IEEE Transactions on Vehicular Technology*, vol. 56, no. 4, pp. 1924–1934, 2007.

[15] H. Xu, V. Kukshya, and T. S. Rappaport, "Spatial and temporal characteristics of 60-ghz indoor channels," *IEEE Journal on selected areas in communications*, vol. 20, no. 3, pp. 620–630, 2002.

[16] A. M. Sayeed, "Deconstructing multiantenna fading channels," *IEEE Transactions on Signal processing*, vol. 50, no. 10, pp. 2563–2579, 2002.

[17] R. W. Heath, N. Gonzalez-Prelcic, S. Rangan, W. Roh, and A. M. Sayeed, "An overview of signal processing techniques for millimeter wave MIMO systems," *IEEE journal of selected topics in signal processing*, vol. 10, no. 3, pp. 436–453, 2016.

[18] S. Han, I. Chih-Lin, Z. Xu, and C. Rowell, "Large-scale antenna systems with hybrid analog and digital beamforming for millimeter wave 5G," *IEEE Communications Magazine*, vol. 53, no. 1, pp. 186–194, 2015.

[19] A. M. Elbir, "CNN-based precoder and combiner design in mmWave MIMO systems," *IEEE Communications Letters*, vol. 23, no. 7, pp. 1240–1243, 2019.

[20] E. Björnson, J. Hoydis, and L. Sanguinetti, "Massive MIMO networks: Spectral, energy, and hardware efficiency," *Foundations and Trends in Signal Processing*, vol. 11, no. 3-4, pp. 154–655, 2017.

[21] R. Eberhart and J. Kennedy, "Particle swarm optimization," in *Proceedings of the IEEE international conference on neural networks*, vol. 4. Citeseer, 1995, pp. 1942–1948.

[22] M. Dorigo, V. Maniezzo, and A. Colorni, "The ant system: An autocatalytic optimizing process," 1991.

[23] D. Karaboga and B. Akay, "A comparative study of artificial bee colony algorithm," *Applied mathematics and computation*, vol. 214, no. 1, pp. 108–132, 2009.

[24] Z. Xiao, H. Dong, L. Bai, D. O. Wu, and X.-G. Xia, "Unmanned aerial vehicle base station (uav-bs) deployment with millimeter-wave beamforming," *IEEE Internet of Things Journal*, vol. 7, no. 2, pp. 1336–1349, 2019.

[25] S. Khalid, W. B. Abbas, H. S. Kim, and M. T. Niaz, "Evolutionary algorithm based capacity maximization of 5g/b5g hybrid pre-coding systems," *Sensors*, vol. 20, no. 18, p. 5338, 2020.

[26] D. Karaboga, "An idea based on honey bee swarm for numerical optimization," Citeseer, Tech. Rep., 2005.

[27] H. Li, M. Li, Q. Liu, and A. L. Swindlehurst, "Dynamic hybrid beamforming with low-resolution PSs for wideband mmWave MIMO-OFDM systems," *IEEE Journal on Selected Areas in Communications*, vol. 38, no. 9, pp. 2168–2181, 2020.

[28] D. H. Nguyen, L. B. Le, T. Le-Ngoc, and R. W. Heath, "Hybrid MMSE precoding and combining designs for mmWave multiuser systems," *IEEE Access*, vol. 5, pp. 19 167–19 181, 2017.